THE ASTROPHYSICAL JOURNAL, 422:111–117, 1994 February 10

RADIAL VELOCITIES OF M GIANTS AT 300 PARSEC PROJECTED RADIUS FROM THE GALACTIC CENTER

R. D. BLUM,[1] J. S. CARR,[1,2] D. L. DEPOY, K. SELLGREN,[3] AND D. M. TERNDRUP[4]
Department of Astronomy, The Ohio State University, 174 West 18th Avenue, Columbus, OH 43210
Received 1993 May 10; accepted 1993 August 17

ABSTRACT

We present radial velocities for 33 stars in an optically obscured field toward the Galactic bulge at $l = -1.^{\circ}14$, $b = 1.^{\circ}81$. The radial velocities are derived from spectra of the 2.3 μm CO bandhead that is prominent in late-type giants. The heliocentric radial velocity and dispersion are -75 ± 24 km s^{-1} and 127 ± 16 km s^{-1}, respectively. Comparison to the axisymmetric mass model of Kent (1992) shows good agreement with the velocity dispersion, but there is some evidence (at the 2.1 σ level) for a more negative mean velocity. The more negative mean velocity is suggestive of streaming motion in a rotating barred potential such as derived by Binney et al. (1991).

Subject headings: Galaxy: center — Galaxy: kinematics and dynamics — stars: giants — techniques: radial velocities

1. INTRODUCTION

Kinematic studies of stars in the inner Galaxy have been used to derive the mass distribution within 1000 pc of the Galactic center (Kent 1992; Lindqvist, Habing, & Winnberg 1992; Sellgren et al. 1990; McGinn et al. 1989; Rieke & Rieke 1988). The most detailed model (Kent 1992) utilizes the kinematic data from all these papers as well as kinematics in "Baade's window" (BW) and several other fields along the bulge minor axis from Rich (1990), Sharples, Walker, & Cropper (1990), and Terndrup, Frogel, & Wells (1994). These data represent a large number of observations of individual stars in the inner Galaxy. However, they are concentrated either near the Galactic center (projected radius $R \lesssim 10$ pc) or in low-obscuration optical windows at $R \gtrsim 400$ pc along the minor axis. An exception is the OH/IR star investigation of Lindqvist et al. that measured 134 sources concentrated toward the Galactic plane extending to approximately $R = 100$ pc. A gap therefore exists in the observations at intermediate distances and in off-axis positions. The minor axis data ($R \gtrsim 400$ pc) sample only the inner Galaxy velocity dispersion; Kent's model relies primarily on these data for the mass distribution at larger radii ($R \gtrsim 100$ pc). Mean velocities are available only near the Galactic center ($R \lesssim 10$ pc) or on the major axis. Thus, as Kent points out, the mass models have not yet been adequately tested for mean velocities in the inner Galaxy due to a lack of observational data.

We have obtained radial velocities for a sample of late-type giants in a single field located at $l = -1.^{\circ}14$, $b = 1.^{\circ}81$ using the 2.3 μm CO bandband. This is the first investigation of kinematics in this region of the inner Galaxy. These data begin to fill the observational gap that exists between the stars of the bulge minor axis fields and those of the Galactic center.

[1] Visiting Astronomer, Cerro Tololo Inter-American Observatory, National Optical Astronomy Observatories, which are operated by the Association of Universities for Research in Astronomy, Inc., under cooperative agreement with the National Science Foundation.

[2] Visiting Astronomer at the Infrared Telescope Facility, operated by the University of Hawaii under contract with the National Aeronautics and Space Administration.

[3] Alfred P. Sloan Research Fellow.

[4] Presidential Young Investigator.

2. OBSERVATIONS AND DATA REDUCTION

2.1. *Imaging*

The program stars were selected from the brighter stars on a K-band ($\lambda = 2.2$ μm, $\Delta\lambda = 0.4$ μm) image (Fig. 1) of the field obtained with the Ohio State Infrared Imaging System (OSIRIS) on the Perkins 1.8 m telescope near Flagstaff, Arizona during 1992 May. OSIRIS is described by Atwood et al. (1993). The scale in Figure 1 is $1.''6$ pixel^{-1}. The brightest stars on the image were saturated since the response of the camera's 256 × 256 NICMOS array becomes nonlinear for stars with $K \lesssim 8.5$ mag at the minimum integration time. In addition to the image shown in Figure 1, we obtained J ($\lambda = 1.25$ μm, $\Delta\lambda = 0.3$ μm) and K images of the field with a 10% transmission neutral density filter yielding stellar images in the linear region for all but one of the program stars. These images were obtained in 1993 March.

J and K magnitudes were derived from synthesized apertures (3 pixel radius) on the image shown in Figure 1 or from images taken with the neutral density filter. The overall flux calibration was obtained from images taken with OSIRIS on the CTIO 4 m telescope during 1993 July. The $0.''4$ pixel^{-1} scale resulted in a much smaller field of view. Seven stars common to the large and small fields were used along with the flux standard HD 161743 (Elias et al. 1982) to calibrate the photometry. The flux standard and seven calibration stars were observed at the same airmass, so no airmass correction was needed. The typical photometric uncertainty for the seven stars in the small field was 0.03 and 0.02 mag at J and K, respectively. Comparison of these magnitudes to the instrumental magnitudes in the larger field results in an uncertainty of 0.06 mag in both J and K. K magnitudes were obtained from Figure 1 by comparing a small set of stars whose response was linear on the image to the same stars from the neutral density filter frames. The $J-K$ color and K magnitude of each program star are given in Table 1.

2.2. *Spectra*

The spectroscopic observations were made on the CTIO 1.5 m telescope during the nights of 1992 July 27 and 28 using the facility infrared spectrometer (IRS) which employs an SBRC

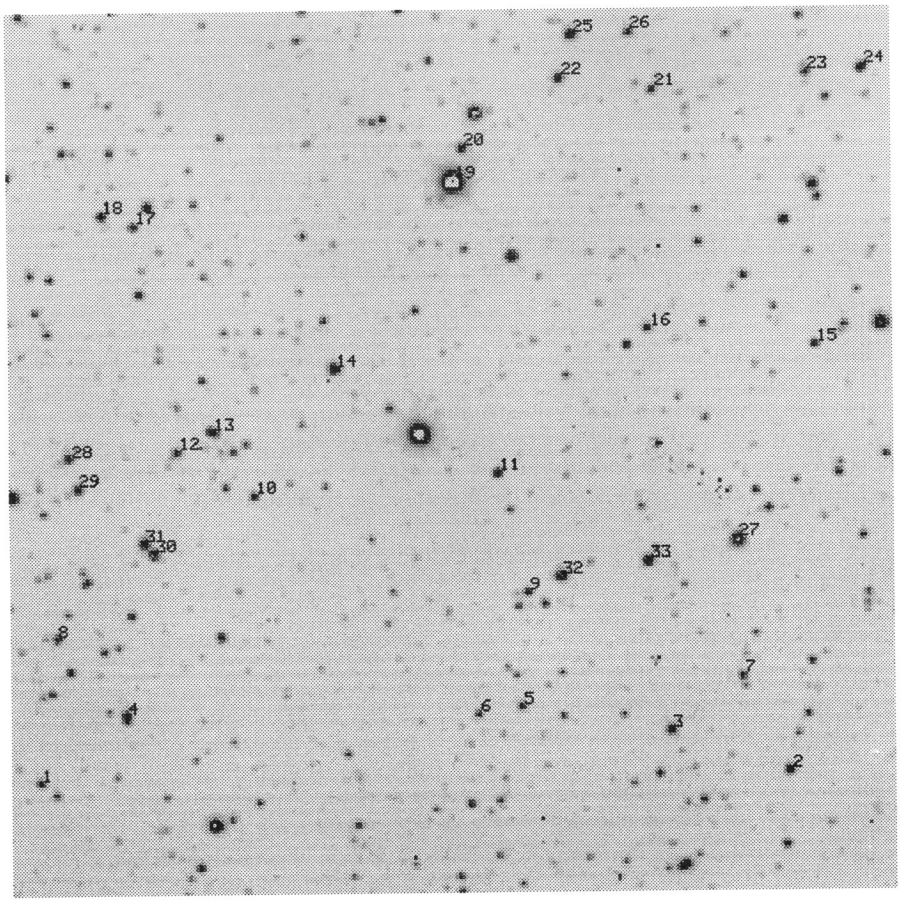

FIG. 1.—42 arcmin^2 2.2 μm image of the off-axis field at $l = -1\overset{\circ}{.}14$, $b = 1\overset{\circ}{.}81$. The numbers correspond to the stars in Table 1. The bright star at center is SAO 185534. The offsets in Table 1 are relative to this star and were determined from this image after a $1\overset{\circ}{.}9$ rotation of the field; see discussion in text. North is up, east to the left.

58 × 62 InSb detector. The IRS is described by DePoy et al. (1990). The 4″.8 × 30″ ($\alpha \times \delta$) slit and 632 lines mm^{-1} grating combined to give a spectral resolution of 84 km s^{-1} at 2.2935 μm, the rest wavelength of the CO 2–0 vibrational-rotational bandhead. The spectrometer was used in first order. The IRS spectra are Nyquist sampled, giving a total spectral coverage of approximately 2600 km s^{-1} (0.02 μm) at 42 km s^{-1} pixel^{-1}. The spatial scale along the slit is 2″.39 pixel^{-1}.

We obtained spectra for 33 stars brighter than about $K = 9.0$ in the 42 arcmin^2 field shown in Figure 1. The field is centered on SAO 185534, located at $\alpha(1950) = 17^h32^m39\overset{s}{.}1$, $\delta(1950) = -28°54'43''$. The locations of the program stars relative to SAO 185534 are shown in Table 1. The program stars were usually observed in a sequence of star-sky-sky-star, where the sky position was chosen from a blank point on the K-band image. All reduction steps were done using IRAF.[5]

The final spectra were obtained through the following procedure. The average of the two star frames was subtracted from the average of the two sky frames. After being divided by dome flat-field images, the spectra were extracted from the images by synthesizing two-dimensional apertures, approximately 3 pixels wide, and collapsing the spatial dimension to form one-dimensional spectra using IRAF "apextract." The spectra were wavelength calibrated by a Xe arc lamp image. In order to correct for the instrumental profile and telluric absorption, early-type stars were chosen from the Bright Star Catalog and observed throughout the night. The program star spectra were then ratioed by these atmospheric standards.

A typical program star spectrum is shown in Figure 2. This spectrum, like all the program stars, shows the strong CO absorption characteristic of K and M giants (Kleinmann &

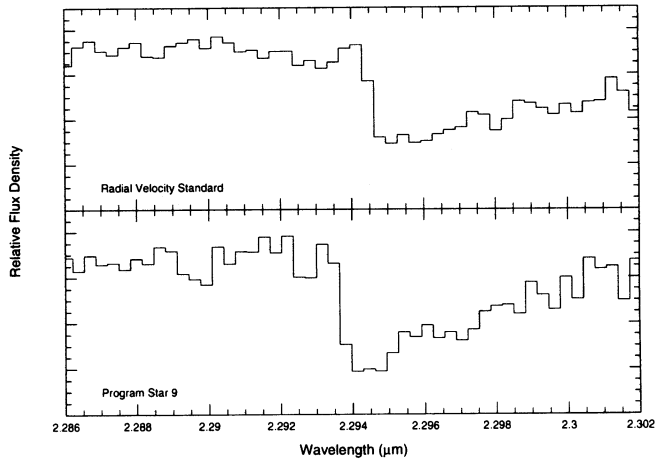

FIG. 2.—Spectra near the 2.3 μm CO bandhead. Points are plotted every 42 km s^{-1}; the spectral resolution is 84 km s^{-1}. *Top:* Radial velocity standard taken from Sharples et al. *Bottom:* Program star 9.

[5] IRAF is distributed by the National Optical Astronomy Observatories.

TABLE 1

PROGRAM STAR POSITIONS AND MEASURED PROPERTIES

Star	$\Delta\alpha$	$\Delta\delta$	V_r (km s^{-1})	K	$J-K$	CO
1.....	174″	−147″	140	8.71	...	0.31
2.....	−157	−155	−117	8.22	2.16	0.46
3.....	−105	−135	−126	8.19	2.19	0.36
4.....	135	−119	112	8.00	2.10	0.33
5.....	−40	−122	−315	8.91	2.15	0.30
6.....	8	−120	−158	9.22	1.98	0.33
7.....	−138	−112	−243	8.80	2.08	0.36
8.....	165	−84	−163	8.55	...	0.33
9.....	−45	−72	−7	8.68	2.20	0.31
10.....	75	−24	1	8.72	2.20	0.33
11.....	−34	−19	−80	8.20	2.22	0.39
12.....	108	−3	125	8.58	2.12	0.32
13.....	92	5	−224	7.93	2.18	0.27
14.....	37	31	−94	7.26	1.86	0.28
15.....	−176	33	−33	8.72	2.17	0.35
16.....	−102	43	130	8.69	2.11	0.40
17.....	123	98	−175	8.80	1.93	0.35
18.....	137	103	106	8.43	2.20	0.28
19.....	−16	115	−57	6.00	...	0.31
20.....	−24	126	−131	8.15	2.30	0.26
21.....	−109	149	41	8.77	2.12	0.35
22.....	−68	156	134	8.11	2.07	0.30
23.....	−177	154	−140	8.53	1.95	0.26
24.....	−202	155	1	7.69	...	0.35
25.....	−74	175	−225	7.61	2.16	0.31
26.....	−100	175	14	8.68	1.51	0.31
27.....	−139	−52	−27	6.50	2.17	0.34
28.....	157	−4	−42	8.09	2.09	0.29
29.....	153	−18	−222	8.24	2.28	0.32
30.....	120	−47	−205	7.43	2.05	0.34
31.....	124	−43	−95	7.50	2.29	0.31
32.....	−60	−65	−135	7.45	2.31	0.32
33.....	−99	−60	−271	7.60	2.16	0.36

NOTE.—All offsets are from SAO 185534 located at $\alpha(1950) = 17^h32^m39^s.1$, $\delta(1950) = -28°54'43''$. The offsets were determined from the K-band image in Fig. 1 and have been corrected for a 1°.9 counterclockwise rotation of the field. The offsets are uncertain by approximately ±1″.5. The radial velocities, V_r, are heliocentric and have individual uncertainties of approximately ±20 km s^{-1}. The K magnitudes and $J-K$ color are observed, not reddening corrected. The photometric errors in the J and K magnitudes are 0.06 mag. The K magnitude for star 19 is an upper limit. No J magnitudes were available for stars 1, 8, 19, and 24; see text. CO absorption strength is the relative flux in 0.005 μm bandpasses just shortward and longward of the bandhead.

Hall 1986). The CO absorption strength was computed by comparing the flux just shortward of the bandhead to the flux longward of the band minimum in 0.005 μm bandpasses. The CO values are given in Table 1. The mean CO absorption strength for the sample is 33% ± 4%.

2.3. *Radial Velocities*

The program stars were cross-correlated with the spectra from a single M8 III star of known radial velocity from "Baade's window" (Sharples et al. 1990, star 301 in their Table 1), using the fast Fourier transform technique employed by the "RV0" package in IRAF. Sharples et al. estimate the error in an individual star to be ±9 km s^{-1}. Observations of this star were made at roughly equal intervals 3 times each night. A spectrum of the velocity standard is shown in Figure 2. Cross-correlation of the multiple spectra of this star taken at different times on each night and between nights showed velocity differences of less than 10 km s^{-1}. This is equivalent to an error in reproducing the standard velocity of 0.12 pixels, or 0.06 of a resolution element.

There are at least three sources of systematic uncertainty in the measurement of these radial velocities. These are shifts in wavelength along the spatial dimension of the slit, wavelength shifts due to observing stars at different positions across the dispersion dimension of the slit, and the uncertainty in the velocity of our standard.

The first two effects could be ignored if each star was precisely placed in the same position in the slit. This was not the case since the program stars are located in an obscured field, and we had no visual counterpart to aid in acquisition and guiding. Program stars were acquired by offsetting from SAO 185534. Uncertainties in the telescope pointing and our calculated offsets resulted in stars being placed at different positions in the slit.

Initially, before any spectra were obtained, we offset to a number of stars at the edge of the field. Comparison of the calculated offset from Figure 1 to the actual offset found by acquiring stars in the slit indicated that the image was rotated approximately 1°.9 counterclockwise. We have corrected for this rotation in the offset values given in Table 1. Each program star was acquired by first centering on the foreground SAO star, using a dichroic in the optical path allowing visual acquisition and guiding, and then offsetting by the amount indicated in Table 1. We relied on the calculated offsets to put the program stars in the slit in order to maximize observing efficiency and, thus, the number of stars obtained.

Consider displacements along the spatial dimension of the slit. Positions in this direction were measured off the two-dimensional spectral images using the "apcenter" routine in IRAF. On the first night, the mean position of the program stars along the slit varied from that of the mean radial velocity standard position by only 0″.45 ± 1″.49. On the second night the difference was 0″.05 ± 1″.50. The relatively small displacements from slit center also indicate that our calculated offsets were uncertain by only ±1″.5 in declination. Throughout each night, OH airglow lines were observed in second order by changing the order sorting filter; the grating was not moved. Comparison of OH spectra separated by more than 10″ above and below the slit center showed shifts of no more than a few km s^{-1}. Therefore, we are confident that there is no significant uncertainty in the radial velocity due to position along the spatial direction.

Next, consider displacements across the slit. A star which is observed alternately at each side of the slit will show a velocity difference due to the different incident angles on the grating. The difference is of order, but less than, the resolution. For the IRS, the 4″.8 slit results in a calculated shift of 72 km s^{-1} for a point source. Observations of star 28 near either side of the slit showed a 42 km s^{-1} shift. We also stepped a bright star across the slit. These spectra show a 32 km s^{-1} shift. The difference in these two measurements indicates the difficulty of precise positioning within the slit. These measured velocity shifts are smaller than the calculated 72 km s^{-1} shift since the stars have finite width and could not be precisely located at the slit edge.

As long as the program stars were placed randomly in the slit with respect to the standard, no large systematic uncertainty is expected since the majority of stars would not be expected to fall at the slit edge. Only in the case where the majority of program stars were observed on the opposite side of the slit from the standard would there be a large systematic error in the mean velocity for the sample. This is unlikely because the standard was placed in the slit by centering its visual counterpart on the marked boresight on the TV guider

while the program stars were placed in the slit by offsetting from SAO 185534 after its visual counterpart was similarly centered on the TV guider. The TV guider reference for the slit was defined by observing a star (usually SAO 185534) on the visual display while peaking up the counts in the spectrometer. This alignment procedure was used to account for differences in the optical and infrared light paths such as might be caused, for example, by differential refraction. The alignment would systematically drift throughout the night until stars were no longer acquired in the slit and the boresight had to be redefined. Alignment was done 2–3 times per night. Since program stars and the standard were obtained at various times after realignment, with no preference for observing the standard right before or after realignment, we expect no systematic differences in the positions in the slit.

Finally, we consider uncertainties in the velocity of our standard. We obtained spectra of a sample of K giants from the Bright Star Catalog (taken as part of a different program on the same nights as the bulge stars with the same setup) with known velocities that we attempted to use to verify the velocity of our standard. The K giants (Bright Star numbers 224, 296, 489, 8841, and 8924) cross-correlate with each other to a mean difference between measured and Bright Star Catalog velocities of 1.3 ± 16 km s^{-1}. However, the K giants cross-correlate with our standard to a mean difference between measured and Bright Star Catalog velocities of -41 ± 10 km s^{-1}, 4 times the uncertainty given by Sharples et al. (1990). We believe this systematic blue shift is due to either declination-dependent instrument flexure or a significant shift in the boresight alignment with declination. The latter seems most likely as we also observed shifts in the boresight alignment while tracking our bulge field in hour angle. Since we did not originally intend to use the K giant velocities, we did not realign the boresight later in the night when the K giant spectra were obtained. The K giants were 20°–30° farther north than the radial velocity standard and program stars. This suggestion, that the difference in calculated velocities between the K giants and the Sharples et al. star was due to declination-dependent flexure and/or boresight shift, was checked by comparing both the K giants and the standard to a spectrum of the M2 supergiant, IRS 7, located near the Galactic center. IRS 7 is less than 1° away from the standard and program stars. The radial velocity of IRS 7 (adjusted to the heliocentric frame of reference) was taken from Sellgren et al. (1987). Cross-correlation with IRS 7 gives a mean difference of -32 ± 8 km s^{-1} for the K giants and 0.0 km s^{-1} for the velocity standard, in agreement with our supposition that the difference in velocities is due to flexure of the instrument and/or boresight shift.

We therefore take the heliocentric velocities for the program stars relative to the star from Sharples et al. to be correct and adopt an uncertainty in an individual measurement of ± 20 km s^{-1}, which is consistent with the analysis of the K giants and the systematic uncertainty due to split positioning as determined from the measurements of star 28.

Subsequent to these observations, we obtained 27 km s^{-1} resolution spectra (3.34 km s^{-1} pixel^{-1}) of four of our program stars using the CSHELL spectrometer (Tokunaga et al. 1990) at the NASA Infrared Telescope Facility on Mauna Kea. The difference between the CSHELL velocities and those reported above is consistent with the quoted uncertainties.

3. THE DISTRIBUTION OF STARS ALONG THE LINE OF SIGHT

To use the measured kinematics in a study of the inner Galaxy, we first need to estimate their distribution in space along the line of sight. In addition, a comparison of the observed kinematics to those predicted by the axisymmetric mass model of Kent (1992) requires not only that the stars be distributed along the line of sight at true galactocentric distances close to the projected radius, but that they also be uncontaminated by disk stars since these are not included in the model. The mean position can be estimated from our photometry and the spatial distribution and contamination can be estimated by construction of a bulge + disk galaxy model.

First of all, an estimate of the extinction to our field will be required for any photometric distance determination. This can be obtained from the J and K photometry of stars in our field. The mean $J-K$ for stars in the field as determined from aperture photometry was 2.11 ± 0.09. The mean intrinsic $J-K$ can be estimated from the measured CO absorption strengths which are independent of reddening. Direct comparison of our mean CO strength with the disk M giant spectra in Kleinmann & Hall (1986) suggests a mean spectral type of M7 or later. The flux in the band and continuum for the Kleinmann & Hall spectra are summed over the same bandpasses used in § 2.2; the resolution of the Kleinmann & Hall spectra is 106 km s^{-1}. Binning our spectra to this smaller resolution does not change the assignment of a mean spectral type for the program stars. The CO strength can also be compared to the spectra of bulge M giants from Ternup, Frogel, & Whiteford (1991). Binning our spectra to wavelength bins 0.0023 μm wide, corresponding to the 300 km s^{-1} resolution of the Terndrup et al. data, results in a mean CO strength of $26\% \pm 3\%$. Using the Terndrup et al. M6–M9 bulge giants (see their Table 5), we find a mean CO strength of $27\% \pm 2\%$. The mean CO strength for the three M6 and three M7 stars is $26\% \pm 3\%$, each separately and for the six stars combined. Here the CO absorption strengths are computed by comparing the flux shortward of the bandhead and longward of the band minimum, in bandpasses approximately 0.006 μm wide.

Assignment of a mean spectral type is uncertain since the spectra all have different original resolutions and the comparison samples are small. We adopt a mean spectral type of M7 III; this corresponds to an intrinsic $J-K$ of 1.15 for the bulge stars in Terndrup, Frogel, & Whitford (1990) which were measured on the CTIO/CIT system. Color transformations between OSIRIS and CTIO/CIT do not yet exist, but we estimate that the correction for an M7 III would result in a $J-K$ bluer by 0.04 mag based on transformations of other NICMOS cameras (Rayner 1993). Since this correction is small and uncertain, we ignore it. Assuming the interstellar reddening curve of Mathis (1990) leads to $A_K = 0.59 \pm 0.06$, where the error is due to the photometric uncertainty.

An estimate of the positions and number of intervening disk stars was made by constructing a disk model based on the luminosity function of Garwood & Jones (1987). The luminosity function is subdivided by spectral class and is defined by star counts in the solar neighborhood. An exponential density distribution was taken in both the radial and disk normal directions. The vertical scale height for each class (the K and M giants have vertical scale heights between 200 and 300 pc) was also taken from Garwood & Jones. A radial scale length of 3 kpc was adopted from Kent, Dame, & Fazio (1991), together with a Sun–to–Galactic center distance of 8 kpc.

A bulge model was also constructed in order to estimate the distribution of positions of bulge stars and the ratio of bulge to disk stars in the field. The space density distribution was adopted from Kent (1992), and the luminosity function was taken from Frogel & Whitford (1987). The bulge model was

normalized such that the total number of stars from the bulge and disk combined, with $K \lesssim 9.0$ mag, equaled the number obtained from the 2.2 μm image of "Baade's window" presented by DePoy et al. (1993). DePoy et al. find 483 stars in their image with $K \leq 9.0$ mag. The normalization does not depend heavily on extinction since the reddening toward Baade's window at K is small ($A_K = 0.14$ mag; Frogel & Whitford 1987).

The total number of stars in our frame brighter than $K = 9.0$ as determined from aperture photometry was 72 ± 9, where the uncertainty arises from the photometric error for a single star. Taking into account the small amount of extinction to BW and the extinction to our field, the bulge + disk model predicts 60 stars brighter than $K = 9.0$ and disk contamination [disk stars/(disk + bulge stars)] of 29%. Allowing for variations in the disk scale length (2500–3500 pc) and Sun–to–Galactic center distance (7500–8500 pc), the disk contamination in our field was predicted to vary from 21% to 47%, with the shortest scale length giving the largest disk contribution. Since the models are normalized by star counts toward BW, changing these parameters does not change the total number of stars predicted by more than a few.

The preferred model is in good agreement with the observed star counts to our field if the extinction toward BW and the field are accounted for. The bulge model predictions do not depend sensitively on the distribution of extinction along the line of sight since most of it is likely to arise in the disk. The measured extinction is less than that determined from the axisymmetric model of Kent et al. (1991) which relies on the radial distribution of gas in the Galactic disk. The smaller amount of extinction measured here may reflect the patchy nature of extinction toward the Galactic center. It also suggests that the distribution of absorbers along our line of sight is different than the azimuthally averaged radial distribution in the disk. Therefore, the extinction is added at a single radius for the models described above. For radii where the extinction is introduced variously from 3500 to 8000 pc from the Galactic center, the total number of stars and the disk contamination change by a few percent. The model quoted above uses an extinction introduced at 4000 pc, the distance at which the gas distribution peaks in the disk (Burton 1988).

Before using the derived models to predict the radial distribution of stars corresponding to our sample, it is first useful to estimate the distance of the program stars along the line of sight by comparing their color-magnitude diagram to that for the M giants in "Baade's window." In Figure 3, we compare the K versus $J-K$ diagram for the program stars to the mean and median relations for the BW M giants measured by Frogel & Whitford (1987) which we have reddened by the amount calculated for our field. No color corrections were applied to the intrinsic BW colors for consistency with the derived $E(J-K)$. No J magnitudes are available for stars 1, 8, and 24 because the J image was rotated slightly with respect to the K image shown in Figure 1, placing these stars off the J frame. These three stars all showed strong CO absorption indicating they are late type giants; none had K magnitudes which would suggest they were foreground objects. Star 19 was saturated on both J and K images, so its color is undetermined. The majority of our stars lie near the Frogel & Whitford relations, suggesting a mean distance that places them in the inner Galaxy. There are four stars (14, 19, 27, 30) with apparent brightnesses that suggest they are foreground disk giants; see Table 1. One star, 26, has significantly lower intrinsic $J-K$. It may be a foreground star, or the extinction may vary in the field. Its combination of K magnitude and CO strength suggests it is not a foreground star. We consider the effect of removing these five stars from the sample in the next section when we discuss the mean velocity and velocity dispersion of the program stars.

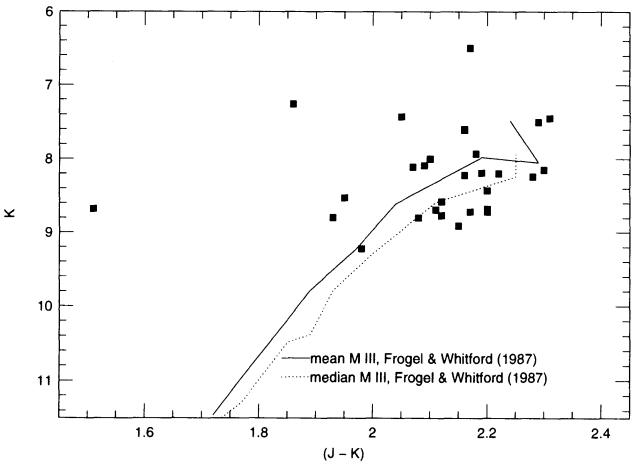

FIG. 3.—Comparison of the K vs. $J-K$ color-magnitude diagram for the program stars (*filled boxes*) and the unbiased sample of "Baade's window" M giants from Frogel & Whitford (1987) which have been corrected to the reddening in our field. Typical uncertainty in K and $(J-K)$ are ± 0.06 and ± 0.09 mag, respectively.

Using the observed magnitudes and colors, an estimate of the distribution of stars along the line of sight can be made from the previously described models. The observed CO strengths indicate that most of the stars are later than about M4–M5 III. Selecting such stars with observed K brighter than 9.0 from the disk + bulge model, we find a distribution highly peaked about the point lying along the line of sight at a true distance from the Galactic center of 300 pc. The distribution is shown in Figure 4, where the distance plotted is the true galactocentric distance to a point along the light of sight. Note that the double lines in this figure result from stars in front and back of the 300 pc point. The mean galactocentric distance to stars along the line of sight is 605, 1815, and 920 pc for the bulge stars, disk stars, and total, respectively. The predicted

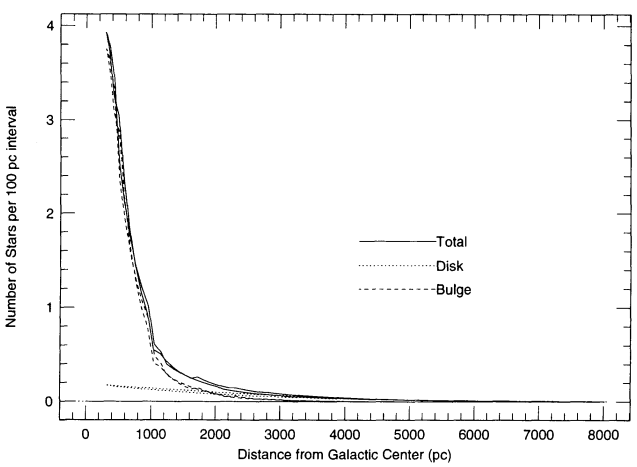

FIG. 4.—Model distribution of stars with respect to true galactocentric distance along the line of sight. The double lines indicate stars in front and back of the point along the line of sight located at 300 pc galactocentric radius.

distribution shows that 50% of the stars are located at true distances less than 400 pc and 90% within 1300 pc. If the short- and long-scale length models are used, the mean distances change up to ±10% for the disk stars and total; the bulge mean distance remains unchanged.

Both Figures 3 and 4 indicate that the program stars are confined to true galactocentric radii near the center of the Galaxy.

4. RESULTS AND DISCUSSION

The resulting velocity dispersion and mean heliocentric radial velocity for the sample of 33 stars are 127 ± 16 km s^{-1} and -75 ± 24 km s^{-1}. The velocities may be corrected to the LSR by adding 10 km s^{-1} to account for Earth's motion through the LSR toward the Galactic center. A further correcton of -4 km s^{-1} may be added to account for the projected component of the 220 km s^{-1} Galactic rotation rate at the solar radius. The quoted error in the dispersion is dominated by statistical uncertainty but includes the effect of a ±20 km s^{-1} systematic uncertainty in an individual measurement (consistent with the observed dispersion in measured K giant velocities and positioning uncertainties discussed in § 2.3). The determination of the statistical uncertainty in the velocity dispersion follows the discussion in Da Costa et al. (1977). The uncertainty in the mean radial velocity is the dispersion added in quadrature to the error for an individual measurement, divided by the square root of the number of stars in the sample, plus the 9 km s^{-1} error in the velocity standard added in quadrature. The distribution of velocities was compared to a Gaussian distribution with the observed mean velocity and velocity dispersion. Application of a Kolmogorov-Smirnov test shows that the distribution is statistically different from a Gaussian at a confidence level of less than 80%; thus there is no statistical evidence that the velocity distribution is non-Gaussian.

The observed kinematics in our field may be compared to Kent's model, for which he reports (private communication) a velocity dispersion of 119 km s^{-1} and mean velocity of -25 km s^{-1} (here we have corrected Kent's mean velocity to the heliocentric frame). The velocity dispersion is in good agreement. If the individual velocities have not been affected in a systematic way, as argued in § 2.3, then there is some evidence (2.1 σ) for larger rotational support than predicted by Kent's model. Indeed, Lindqvist et al. (1992) derive a dynamical model for the inner Galaxy that shows more rotational support (higher mean radial velocities) than Kent's model. They derive the mass distribution from kinematics of OH/IR stars under an assumed spherical potential. At 104 pc, similar to the longitude of our field but along the major axis, they find a mean radial velocity of 97 ± 14 km s^{-1} and dispersion of 111 ± 14 km s^{-1}. The mean radial velocity is much larger than given by Kent's model which predicts a mean radial velocity of 40 km s^{-1} everywhere on the major axis. However, Lindqvist et al. find that a subsample of their stars, which may be less concentrated toward the plane, shows lower mean velocities. The OH/IR stars, in general, are strongly concentrated toward the Galactic plane (approximately within ± 50 pc), so they may not be representative of stars at more extended latitudes.

The Kent dynamical model is a solution to the Jeans equations and as such, requires that the population used to trace the stellar space density distribution is the same as that from which the kinematics are obtained. Since the Kent model has no disk population included, we must account for the possibility that the observed kinematics do include disk stars. Our two component models indicate a disk contribution of 21%–47% of the sample. Disk stars might be identified by their position on the color-magnitude diagram in Figure 3. Stars 14, 19, 27, and 30 have similar color but brighter apparent magnitudes than those on the BW relations and may thus be foreground disk stars. Star 26 has lower intrinsic $J-K$ and may thus be in the foreground. If we remove these five stars (15% of the sample), the mean radial velocity and velocity dispersion are -75 ± 26 km s^{-1} and 134 ± 17 km s^{-1}, respectively. Thus, there is no significant change in the result if these stars are excluded.

While including a dynamical disk model is beyond the scope of the present paper, the effects of contamination can be estimated from the observed disk star kinematics found by Lewis & Freeman (1989). Lewis & Freeman find a radial velocity dispersion of 89.3 ± 9.5 km s^{-1} at a distance of 1400 pc and 94.8 ± 9.0 km s^{-1} at 600 pc from the Galactic center toward BW. They find mean radial velocities less than 20 km s^{-1} toward BW at distances between 5 and 1 kpc from the Galactic center. Thus, we would expect that if stars such as these are, in fact, included in the present sample, removing them (assuming mean kinematics) from the bulge sample would result in an increase in the dispersion and a more negative mean velocity. Thus, we would expect a correction for disk contamination to increase the discrepancy in mean radial velocity between our measurements and the Kent axisymmetric model; the velocity dispersion would still be in good agreement. More importantly, given that the disk increases in temperature toward the center and that most of the stars intervening along the line of sight are expected to be close to the bulge (a consequence of the space distributions assumed in our models along with the magnitude limit), separation of the stars into distinct components cannot be easily done kinematically and would be difficult even with accurate distance indicators.

We believe the velocity dispersion estimate is probably robust, because the kinematics remain essentially unchanged if we exclude the stars most likely to be disk stars, the disk itself increases in temperature at small galactocentric radii, and the stars appear to be distributed close to the point along the line of sight at galactocentric radius 300 pc. The large (negative) mean radial velocity measured here and also those measured by Lindqvist et al. (1992) suggests that the mass distribution still remains uncertain in this region of the inner Galaxy.

An interesting final note is that the large negative mean velocity found for this sample is suggestive of the streaming motions of stars moving in a barred potential seen at a small angle relative to its major axis. Binney et al. (1991) infer a rotating bar from the inner Galaxy gas kinematics which has a major axis inclined to our line of sight by $16° \pm 2°$. Blitz & Spergel (1991) derive strong evidence for a nuclear bar from asymmetries in the 2.4 μm surface brightness distribution in the first and fourth Galactic quadrants. This near infrared surface brightness distribution asymmetry is confirmed by the *COBE* observations of Weiland et al. (1993) who used multicolor data to correct for extinction. The mean velocity found in our sample is in the same sense as the gas moving on closed orbits in the Binney et al. potential, and the longitude and latitude of our field are well within the angular scale lengths of the bar derived by Blitz & Spergel.

Two cautionary notes are in order. The orientation of the bar is well constrained by the gas kinematics, but the analysis of the stellar surface brightness distribution does not tightly

constrain the orientation to be close to the line of sight. Also, since we have measurements in only one field, the large mean radial velocity, which differs from Kent's axisymmetric model only at the 2.1 σ level, could result from systematic errors. Our recent observations in two other fields at similar radii should help resolve these questions as well as the uncertainty in the mass distribution in this region.

5. SUMMARY

We have obtained radial velocities for a sample of 33 late-type stars in a 42 arcmin^2 field distributed near 300 pc projected radius from the Galactic center. Analysis of the 84 km s^{-1} resolution spectra centered on the CO bandhead at 2.3 μm results in a mean velocity of -75 ± 24 km s^{-1} and a dispersion of 127 ± 16 km s^{-1}. Comparison to the axisymmetric mass model of Kent (1992) shows good agreement with the velocity dispersion but some evidence (2.1 σ) for a more negative mean velocity than expected. The large (negative) mean velocity is suggestive of streaming motion in a rotating barred potential such as derived by Binney et al. (1991) for the inner Galaxy.

This work was supported by NSF grant AST-9115236. OSIRIS was built under NSF grant AST90-16112. We thank Mark Wagner and Ray Bertram at Lowell Observatory for their assistance in obtaining the OSIRIS image and Luis Gonzalez at CTIO for his help in obtaining the spectra. We especially thank Stephen Kent for providing calculations of the kinematics along the line of sight to our field and for helpful comments as referee. J. S. C. acknowledges the support of a Columbus fellowship.

REFERENCES

Atwood, B., Byard, P., O'Brien, T., DePoy, D., Frogel, J., Henden, A., & Duemmel, K. 1994, in preparation
Binney, J., Gerhard, O. E., Stark, A. A., Bally, J., & Uchida, K. I. 1991, MNRAS, 252, 210
Blitz, L., & Spergel, D. N. 1991, ApJ, 379, 631
Burton, W. B. 1988, in Galactic & Extragalactic Radio Astronomy, ed. G. L. Verschuur & K. I. Kellerman (New York: Springer-Verlag), 332
Da Costa, G. S., Freeman, K. C., Kalnajs, A. J., Rodgers, A. W., & Stapinski, T. E. 1977, AJ, 82, 810
DePoy, D. L., Gregory, B., Elias, J., Montane, A., Perez, G., & Smith, R. 1990, PASP, 102, 1433
DePoy, D. L., Terndrup, D. M., Frogel, J. A., Atwood, B., & Blum, R. 1993, AJ, 105, 2121
Elias, J. H., Frogel, J. A., Matthews, K., & Neugebauer, G. 1982, AJ, 87, 1029
Frogel, J. A., & Whitford, A. E. 1987, ApJ, 320, 199
Garwood, R., & Jones, T. J. 1987, PASP, 99, 453
Kent, S. M. 1992, ApJ, 387, 181
Kent, S. M., Dame, T. M., & Fazio, G. 1991, ApJ, 378, 131
Kleinmann, S. G., & Hall, D. N. B. 1986, ApJS, 62, 501
Lewis, J. R., & Freeman, K. C. 1989, AJ, 97, 139
Lindqvist, M., Habing, H. J., & Winnberg, A. 1992, A&A, 259, 118
Mathis, J. S. 1990, ARA&A, 28, 37
McGinn, M. T., Sellgren, K., Becklin, E. E., & Hall, D. N. B. 1989, ApJ, 338, 824
Rayner, J. T. 1993, private communication
Rich, R. M. 1990, ApJ, 362, 604
Rieke, G. H., & Rieke, M. J. 1988, ApJ, 330, L33
Sellgren, K., Hall, D. N. B., Kleinmann, S. G., & Scoville, N. Z. 1987, ApJ, 317, 881
Sellgren, K., McGinn, M. T., Becklin, E. E., & Hall, D. N. B. 1990, ApJ, 359, 112
Sharples, R., Walker, A., & Cropper, M. 1990, MNRAS, 246, 54
Terndrup, D. M., Frogel, J. A., & Wells, L. 1994, in preparation
Terndrup, D. M., Frogel, J. A., & Whitford, A. E. 1990, ApJ, 357, 453
———. 1991, ApJ, 378, 742
Tokunaga, A. T., Toomey, D. W., Carr, J. S., Hall, D. N. B., & Epps, H. W. 1990, in Instrumentation in Astronomy VII, Proc. SPIE, 1235, 131
Weiland, J. L. 1993, in Back to the Galaxy, in press